

NOTICE

This report was prepared as an account of work sponsored by an agency of the United States Government. Neither the United States Government nor any agency thereof, nor any of their employees, makes any warranty, express or implied, or assumes any legal liability or responsibility for the accuracy, completeness, or usefulness of any information, apparatus, product, or process disclosed, or represents that its use would not infringe privately owned rights. Reference herein to any specific commercial produce, process, or service by trade name, trademark, manufacturer, or otherwise, does not necessarily constitute or imply its endorsement, recommendation, or favoring by the United States Government or any agency thereof. The views and opinions of authors expressed herein do not necessarily state or reflect those of the United States Government or any agency thereof.

NOTICE

Available from:

National Technical Information Service
U.S. Department of Commerce
5285 Port Royal Road
Springfield, Virginia 22161
703-487-4650

Use the following price codes when ordering:

Price: Printed Copy A03
Microfiche A01

Sawtooth Stabilization by Localized Electron Cyclotron Heating in a Tokamak Plasma

K. Hanada, H. Tanaka,* M. Iida, S. Ide,[†] T. Minami,
M. Nakamura,[‡] T. Maekawa, Y. Terumichi and S. Tanaka

Department of Physics, Faculty of Science
Kyoto University, Kyoto, JAPAN
and

M. Yamada, J. Manickam and R. B. White
Plasma Physics Laboratory, Princeton University
Princeton NJ 08543 USA

Sawtooth oscillations (STO) in the ohmically heated WT-3 tokamak are strongly modified or suppressed by localized electron cyclotron resonance heating (ECH) near the $q = 1$ surface, where q refers to the safety factor. The effect of ECH is much stronger when it is applied on the high field side (the inner side of the tokamak) as compared to the low field side (outer side). Complete suppression of the STO is achieved for the duration of the ECH when it is applied on the high field side, in a low density plasma, provided the ECH power exceeds a threshold value. The STO stabilization is attributed to a modification of the current density profile by hot electrons generated by ECH, which reduces the shear in the $q = 1$ region.

*Present address: Physics Laboratory, College of Liberal Arts and Science, Kyoto University.

[†]Japan Atomic Energy Research Institute, Naka Fusion Research Establishment, Ibaraki-ken, Japan.

[‡]Osaka Institute of Technology, Osaka, Japan

Sawtooth oscillations (STO) in tokamaks have long been the subject of intense study. Recently it has been recognized that they can be stabilized by a variety of means, including: lower hybrid current drive,¹⁻⁴ ICRF heating⁵ and electron cyclotron resonance heating.⁶⁻⁹ Several models¹⁰⁻¹² have been proposed as possible stabilization mechanisms. However, a comparison of these models with experiments has been inconclusive, partly due to the difficulty of monitoring and or controlling the plasma parameters near the $q = 1$ surface, where q refers to the plasma safety factor. In the WT-3 tokamak, STO are observed to be strongly modified and/or stabilized by ECH. The sharply localized nature of the ECH provides an effective tool for modifying plasma parameters locally near the $q = 1$ surface. These observations as well as plausible theoretical explanations for the stabilization are the subject of this letter.

The experiments were carried out in the WT-3 tokamak,¹³ with major and minor radii of $R = 65$ and $a = 20\text{cm}$, respectively. The toroidal field was $B_T \leq 1.75T$, and the plasma current was $I_p \leq 150\text{kA}$. Microwaves from a gyrotron ($\omega/2\pi = 56\text{GHz}$, $P_{ECH} \leq 200\text{kW}$) were transferred through circular waveguides to a Vlasov antenna with an elliptic reflector placed along the major radius and injected into the plasma from the low field side. This sharply focussed wave, propagating as the X-mode with an angle of $\theta = 88^\circ$ to the toroidal field, is absorbed at the second harmonic ECH resonance layer, r_{ECH} .

Sawtooth oscillations were observed when the current was such that the safety factor at the limiter was in the range $q_L = 2.2 \sim 6.0$. The sawtooth period τ_s , as well as the amplitude, increase when the ECH power, P_{ECH} , is applied. These modifications of the STO are very sensitive to the field B_T which determines the location where the ECH is localized. The ECH power is held constant and B_T is adjusted so that the resonance occurs at different surfaces, the geometric configuration is shown in Fig. 1(a), while the changes in the soft X-ray (SXR) signal, I_{sx} due to the ECH are shown in Figs. 1(b)-(d). When the ECH is at the $q = 1$ surface on the high field side, (HFS), Fig. 1(b), the sawtooth oscillations are completely stabilized. When the heating occurs on the low field side (LFS) of the same $q = 1$ surface, τ_s increases enormously, and is greater than the energy confinement time, τ_e , ($\tau_s = 3\text{ms}$, $\tau_e = 1\text{ms}$), and the amplitude saturates, Fig. 1(d). In contrast when the heating occurs away from the $q = 1$ surface, at the magnetic axis,

I_{sx} ramps up sharply and drops deeply during the crash phase, Fig. 1(c). These observations clearly indicate the critical importance of the location of the application of ECH. Other effects are easily excluded, since the plasmas in the ohmically heated phase are essentially similar. [With ECH at $r_{q=1}$ on the LFS, the electron density decreases slightly, $n_e = (7 \rightarrow 6) \times 10^{12} \text{ cm}^{-3}$, and the temperature as measured by Thomson scattering increases, $T_{e\perp}(0) = 510 \rightarrow 670 \text{ eV}$, resulting in a decrease of the loop voltage, $V_L = 1.5 \rightarrow 0.8 \text{ V}$, while the plasma current was held constant at $I_p = 80 \text{ kA}$ ($q_L = 4.3$). There was no change in the OV impurity line emission.]

These results are shown in greater detail in Figs. 2 (a)-(c). Figure 2(a) shows the dependence of τ_s on $r_{2\omega_e}$, which is varied by changing B_T , without and with ECH. In the former case we observe that there is no significant variation at all. On the other hand τ_s has two resonance values when B_T is such that the ECH occurs at $r_{q=1}$, where τ_s increases significantly. When $r_{ECH} = r_{q=1}$ on the HFS, τ_s is increased and complete stabilization is observed. On the other hand when the heating is on the LFS, τ_s is increased substantially but stabilization is not observed. These results are complemented by the corresponding variation in the amplitude, Fig. 2 (b), which shows the peaking of the amplitude when the ECH is on axis and at $r_{q=1}$. In Fig. 2 (c) we show the variation of the inversion radius of the STO with q_L . Inversion radii decrease with increasing q_L and they are always larger with ECH. The $q = 1$ radius can be determined from computer tomographic reconstructed images of SXR emissivity at the crash phase, and also from the measured T_e profiles, and we conclude that $r_{q=1}$ is a little larger than r_{inv} , since the latter is determined by the spatial variation of the SXR signal integrated along the line of sight.

In addition to the influence of B_T , which determines the location of the ECH, other plasma parameters play an important role as well. These include the power of the ECH, P_{ECH} , and the electron density, n_e . The dependence on P_{ECH} is shown in Fig. 3, where we have plotted τ_s as a function of P_{ECH}/P_{OH} . We observe that there is an initial linear phase where τ_s increases linearly, and at larger value of P_{ECH}/P_{OH} there is a rapid non-linear increase resulting in complete stabilization. This occurs at $P_{ECH}/P_{OH} \simeq 3.5$ for the particular set of plasma conditions of Fig 3, $q_L = 3.4$, $n_e = 5 \times 10^{12} \text{ cm}^{-3}$ when the ECH is at $r_{q=1}$ on the HFS. In contrast, τ_s just increases linearly with P_{ECH} when the ECH is on the LFS or at the magnetic axis. The threshold

value decreases when q_L increases. When $q_L \sim 4.7$ the critical power for stabilization is $P_{ECH}/P_{OH} \sim 1$. It is interesting to note that at these high q_L values complete stabilization of the STO is possible even when ECH is applied on the LFS. In this case the threshold power on the LFS is 1.7 times larger than the threshold on the HFS.

The electron density also plays a critical role, as shown in Fig. 4. The period τ , increases abruptly when n_e decreases below $n_e = 6 \times 10^{12} \text{ cm}^{-3}$, complete suppression is obtained when $n_e \sim 5 \times 10^{12} \text{ cm}^{-3}$, and the ECH is at $r_{q=1}$ on the HFS. Concomitantly the X-ray energy spectra shows a high energy tail indicating the presence of a hot electron population with $T_{eh} \simeq 60 \text{ keV}$ extending up to 300 keV , in these low density plasmas. In the absence of ECH, ($T_e \sim 0.5 \text{ keV}$), hot electron tails are not observed. The SXR emission from the thermal electrons above 0.9 keV increases with density regardless of the presence or absence of ECH.

These observations suggest that the high energy tail electrons generated by ECH in the low density regime, may be responsible for the stabilization of the STO. However, it must be noted that these hot electrons are generated equally profusely when the ECH is applied either at the axis or at the LFS of the $q = 1$ surface. As such they cannot account entirely for the stabilization of the sawtooth, but might contribute to the effect. Here, we propose that the stabilization is due to a modification of the current profile in such a manner as to lower the shear at the $q = 1$ surface, thus stabilizing the resistive $m/n = 1/1$ mode.¹⁰ Specifically, we suggest that when ECH is applied, $T_{e\perp}$ increases, ($\delta T_{e\perp}/T_{e\perp} \simeq 0.3$), and the electron collisionality and hence the plasma resistivity is reduced, driving more current in this region. This incremental change of the current density would result in a local reduction of the shear,

$$s = \frac{2}{q} \frac{dq}{d\psi} \frac{V}{dV/d\psi},$$

where ψ refers to the poloidal flux, and V refers to the plasma volume enclosed by the surface. We note that this is the toroidal equivalent of $s = r/q dq/dr$. If this reduction in s occurs at the $q = 1$ surface it will have a stabilizing effect on the $m/n = 1/1$ resistive mode which plays an important role in STO.

We have modelled this using the PEST code. We start with a current profile that smoothly vanishes at the plasma edge with $q_{axis} = 0.83$, and

$q_L = 3.37$, and has the $q = 1$ surface at an average radius of 0.35 of the plasma minor radius, a parabolic pressure profile is chosen. Although q_{axis} could not be measured accurately, the experimental evidence on other devices^{4,5} suggests that q_{axis} is less than unity before and during the sawtooth stabilization period. Furthermore, in the present experiment, we expect $q_{axis} < 1$ due to the absence of an adequate mechanism for broadening the current profile.⁵ We determine the stability of this model equilibrium to the ideal and resistive $m/n = 1/1$ modes. The q -profile is modified locally near the $q = 1$ surface in a manner which reduces the shear at that surface, and a new equilibrium is computed.

The stability limits of such a sequence of equilibria at different values of β_{pol} are shown in Fig. 5(a). In the initial OH phase the plasma is unstable to the resistive mode (A), and as the ECH is applied the shear is reduced and the plasma is at marginal stability at (B), further heating reduces the shear further and stabilizes the mode completely (C). The current profile at this point shows a local peak near the $q = 1$ surface and is associated with a reduction of the local shear as indicated in Fig. 5(b). Thus we attribute the suppression of the sawteeth to a stabilization of the $m/n = 1/1$ mode by profile modification.

To explain the differences when heating on the HFS and LFS, we note that: when ECH is applied on the HFS, the high energy electrons can traverse most of the surface enhancing a locally peaked current profile on the entire surface. In contrast when the ECH is applied on the LFS, many of the high energy electrons are easily trapped in the banana region and do not contribute to an enhancement of the current density. As a result there is a smaller influence on the shear and hence the stability when heating on the LFS.

As indicated earlier, in addition to the effects of the high energy electrons on the shear through the current profile, we might expect an energetic particle stabilization effect as discussed in White et al.^{11,12} Although the stability window discussed in Ref. 12 does not exist in the present experiment, since $\beta_p \ll 1$ and $\omega_A > \omega_e^*$, there is still a stabilizing effect from the high energy electrons which are precessing much faster than the background diamagnetic velocity. Here $\omega_{de} > \omega_e^*/2$, where $\omega_{de} = W_\perp/erRB_T$, and $\omega_e^* = (k_\theta/eB_T)\nabla p/n_0$. This criterion can be written as $W_\perp > R\nabla p/n_0 \sim T_e R/a \sim 1.5 \text{ keV}$ ($T_e = 0.5 \text{ keV}$) and is well fulfilled, since the measured HXR

temperature is $T_{eh} \sim 60\text{keV}$. The stabilization thus takes the form found in Ref. 12, with the resistive kink growth rate asymptotically going to zero as the high-energy electron density, n_h , becomes large. A quantitative estimate of this stabilization would require knowledge of the high-energy electron distribution function, which is not available at present.

In conclusion we have found a clear stabilization of STO due to ECH when it is applied near the $q = 1$ surface. This effect is much stronger when the ECH is applied on the high field side. There is a power threshold above which complete stabilization is obtained, below that the sawtooth period increases linearly. Similarly stabilization occurs only below a density threshold. The stabilization is attributable to a local reduction of the shear near the $q = 1$ surface with some contribution due to energetic particle effects. This latter effect may be similar to that observed with ICRF heating in JET and TFR.¹⁴ These results also suggest that STO may be controlled effectively with ECH at the $q = 1$ surface, especially by application on the high field side.

Acknowledgment

The authors appreciate valuable discussions with Drs. T.K. Chu, A. Kritz, K. McGuire, J. Stevens, W. Stodiek, and W. Tang. One of the authors (M. Yamada) thanks the Japan Society for Promotion of Science for their support during his stay at Kyoto University.

This work was supported by a Grant-in-Aid of Scientific Research from the Ministry of Education in Japan and U. S. Department of Energy, under Contract No. DE-AC02-76CH03073.

References

- ¹F. X. Soldner et al., Phys. Rev. Lett., **57** 1137(1986).
- ²T. K. Chu et al., Nucl. Fusion, **26** 666(1986).
- ³M. Iida et al., J. Phys. Soc. Jpn **57** 3661(1988).
- ⁴JT-60 Team, Plasma Phys. Controlled Fusion **31** 1597(1989).
- ⁵D. J. Campbell et al., Phys. Rev. Lett. **60** 2148(1988).
- ⁶G. A. Bobrovskii et al. Sov. J. Plasma Phys. **13** 665(1987).
- ⁷TFR group, Nucl. Fusion **28** 1995(1988).
- ⁸R. T. Snider et al., Phys. Fluids B1 404(1989)
- ⁹Y. Terumichi et al., Proc. 8th Topical Conf. on RF Power in Plasmas, Irvine, 1989 (AIP) p. 88.
- ¹⁰H. Soltwisch et al., Proc. 10th Int. Conf. on Plasma Phys. and Controlled Nucl. Fusion Res., Kyoto 1986 (IAEA, Vienna, 1987) Vol 1. p.263.
- ¹¹R. B. White et al., Phys. Rev. Lett. **60** 2038(1988)
- ¹²R. B. White et al., Phys. Rev. Lett. **62** 539(1989)
- ¹³H. Tanaka et al., Phys. Rev. Lett. **60** 1033(1988).
- ¹⁴J. C. Hosea et al., in Proceedings of the Joint Varenna-Lausanne International Workshop on Theory of Fusion Plasmas, Varenna, August 27-31, 1990, to be published.

Figure captions

Figure 1. (a) Schematic of the wave trajectory and ECR layers r_{ecr} , shown as vertical lines for the three cases b, c , and d shown below. The $q = 1$ surface is shown as a broken circle. Evolution of the soft X-ray signal, $I_{SX}(0.7\text{keV})$ for (b) ECH at $q = 1$ on the high field side ($B_t = 0.93T$), (c) on-axis heating ($B_t = 1.02T$), and (d) the low field side of $q = 1$ ($B_t = 1.08T$) for $q_L = 3.4$, $I_p = 83 \simeq 100\text{kA}$, and $P_{ECH} = 213\text{kW}$.

Figure 2. (a) The sawtooth period τ_s , and (b) relative amplitude $\Delta A/A$ are plotted vs. r_{ECH} (or B_t) with P_{ECH} , open circles, and without P_{ECH} , crosses for $q_L = 3.4$. Note that τ_s reaches 30ms, the duration of the ECH, when $r_{ECH} = r_{q=1}$ on the high field side. (c) Twice the inversion radius, $2r_{inv}$ as measured by SXR detector arrays for both OH(X) and ECH(O) asmas are plotted as functions of q_L .

Figure 3. τ_s vs. normalized ECH power, P_{ECH}/P_{OH} , for $hq = 1$ surface on the HFS (open circles), low field side (crosses), and for on-axis heating (triangles). Insets are temporal evolution of the SXR signal above 0.75keV for various ECH power values: $P_{ECH} = 46$ (a), 123 (b) and 213kW (c); the ECH was on the HFS, with $I_p = 80\text{kA}$, $B_t = 0.91T$, $n_e = 5 \times 10^{12}\text{cm}^{-3}$ and $q_L = 3.4$.

Figure 4. (a) The sawtooth period τ_s , with P_{ec} (open circles) and without P_{ec} (crosses), are plotted as functions of the bulk electron density, n_e , for ECH at $q = 1$ on the HFS, (b) shows the $I_{SX}(2.5\text{ keV})$ emitted by the high energy electrons generated by ECH.

Figure 5. (a) Stability diagram for the $m/n = 1/1$ mode in WT-3, with respect to the shear, s , and β_{pol} . The two curves show the stability boundaries for the resistive and ideal instability. As the ECH power is increased the shear is reduced and the plasma moves from an unstable point (A), without ECH to a marginal point (B) with ECH at threshold power to a stable point (C) with substantial ECH power; (b) The current density, j , and q profile across the plasma mid-plane without ECH (broken curves) and with ECH (solid curves). The inset shows a magnification of the $q \simeq 1$ region to show the reduction of the shear when the ECH was in use.

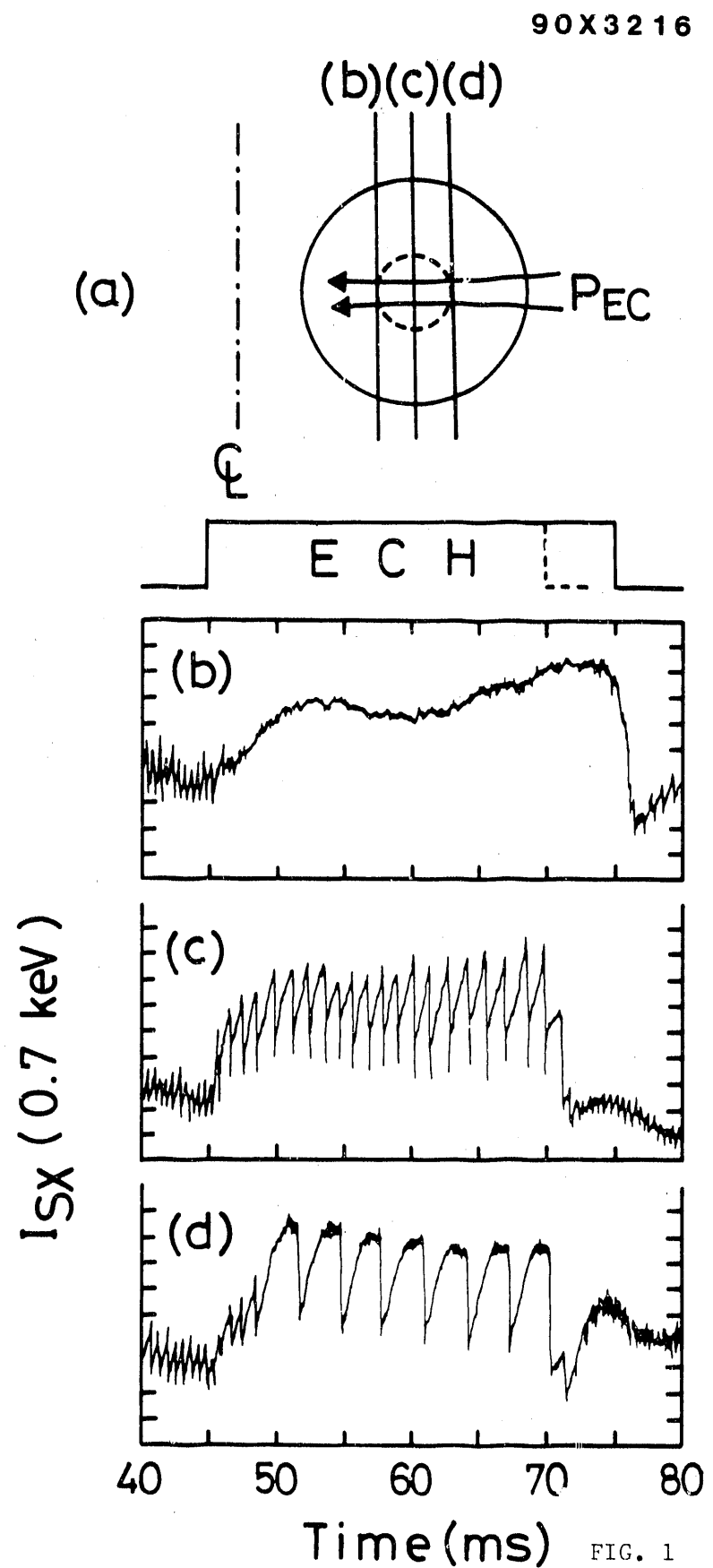


FIG. 1

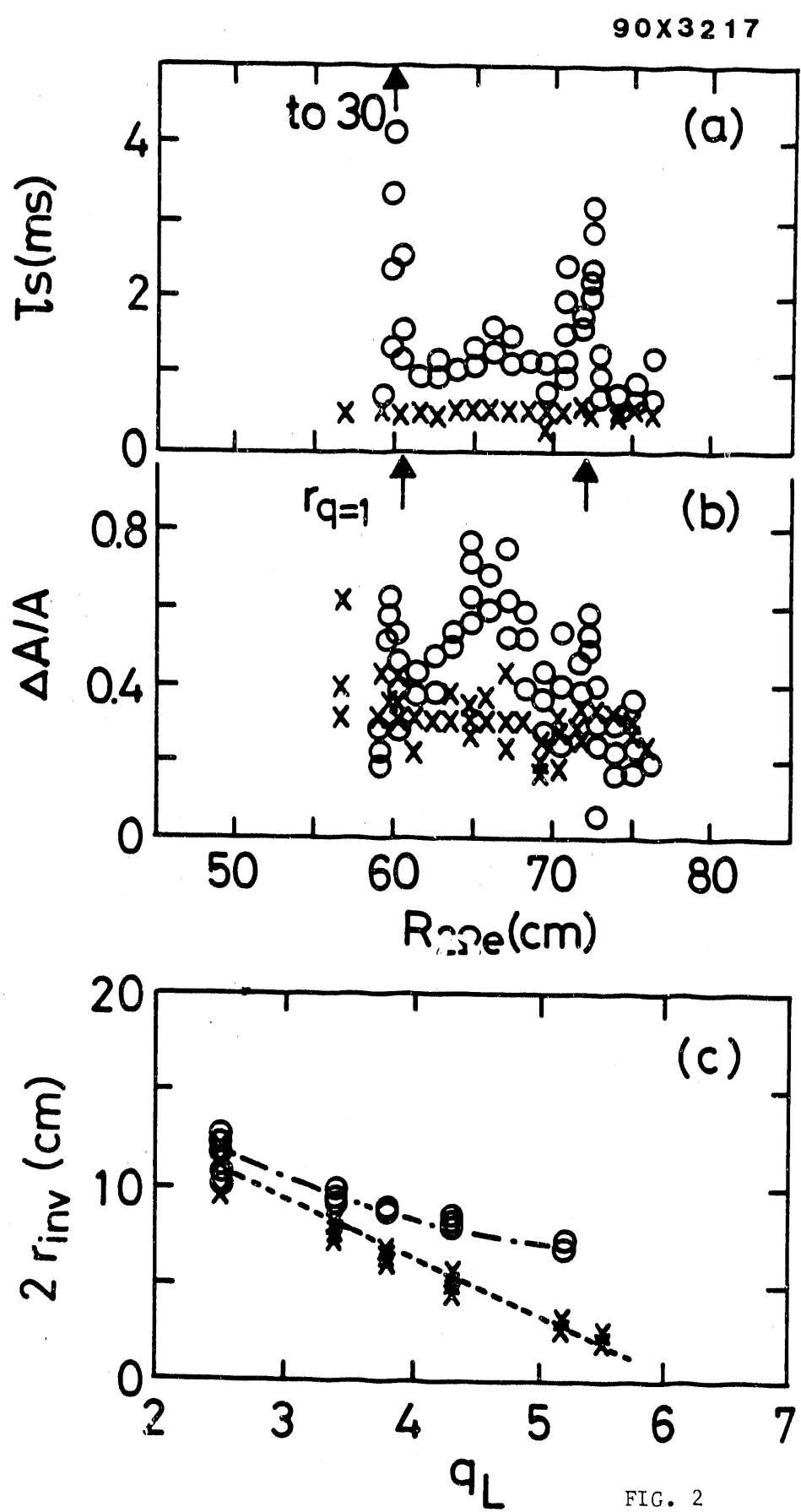


FIG. 2

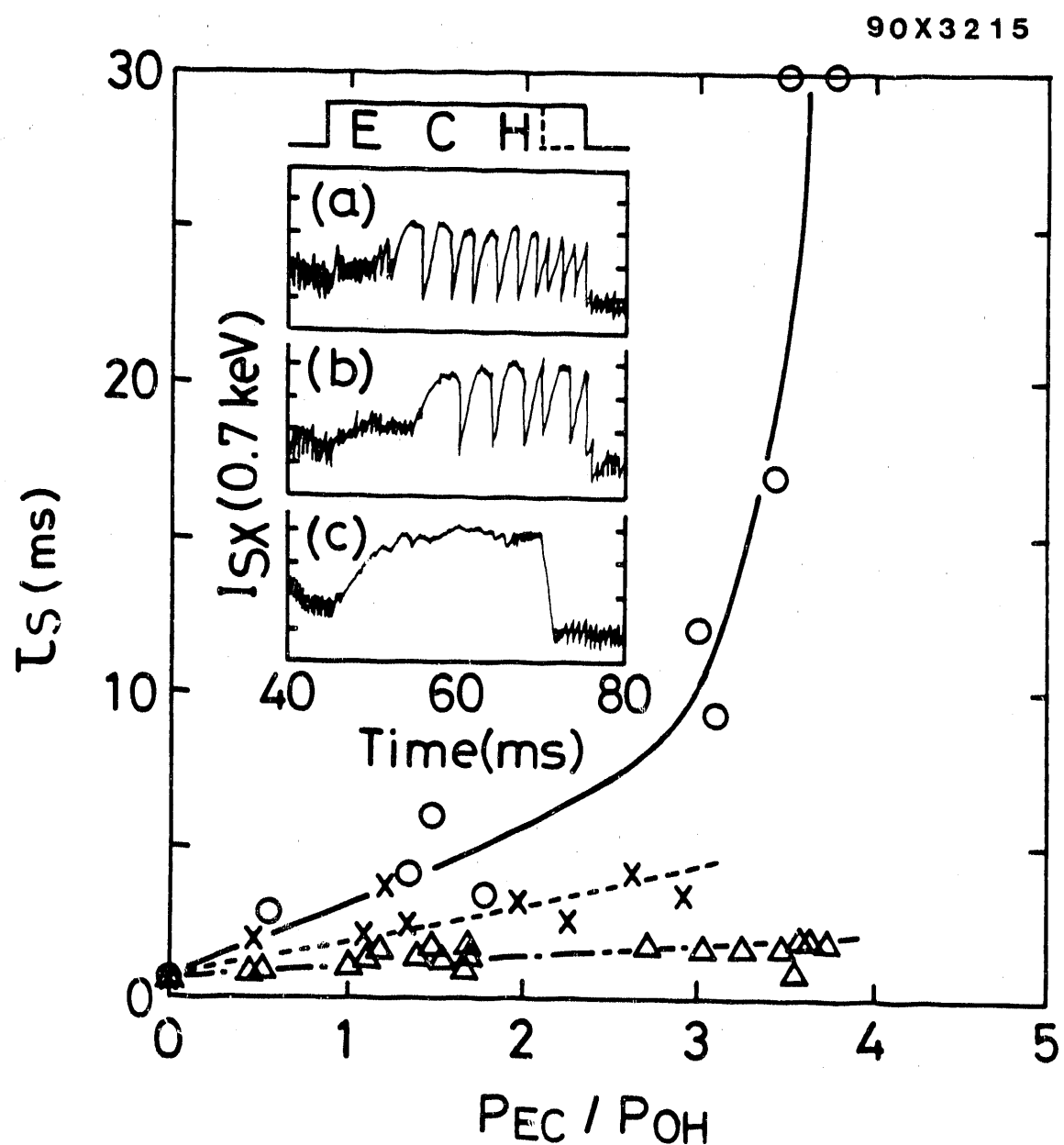


FIG. 3

90X3219

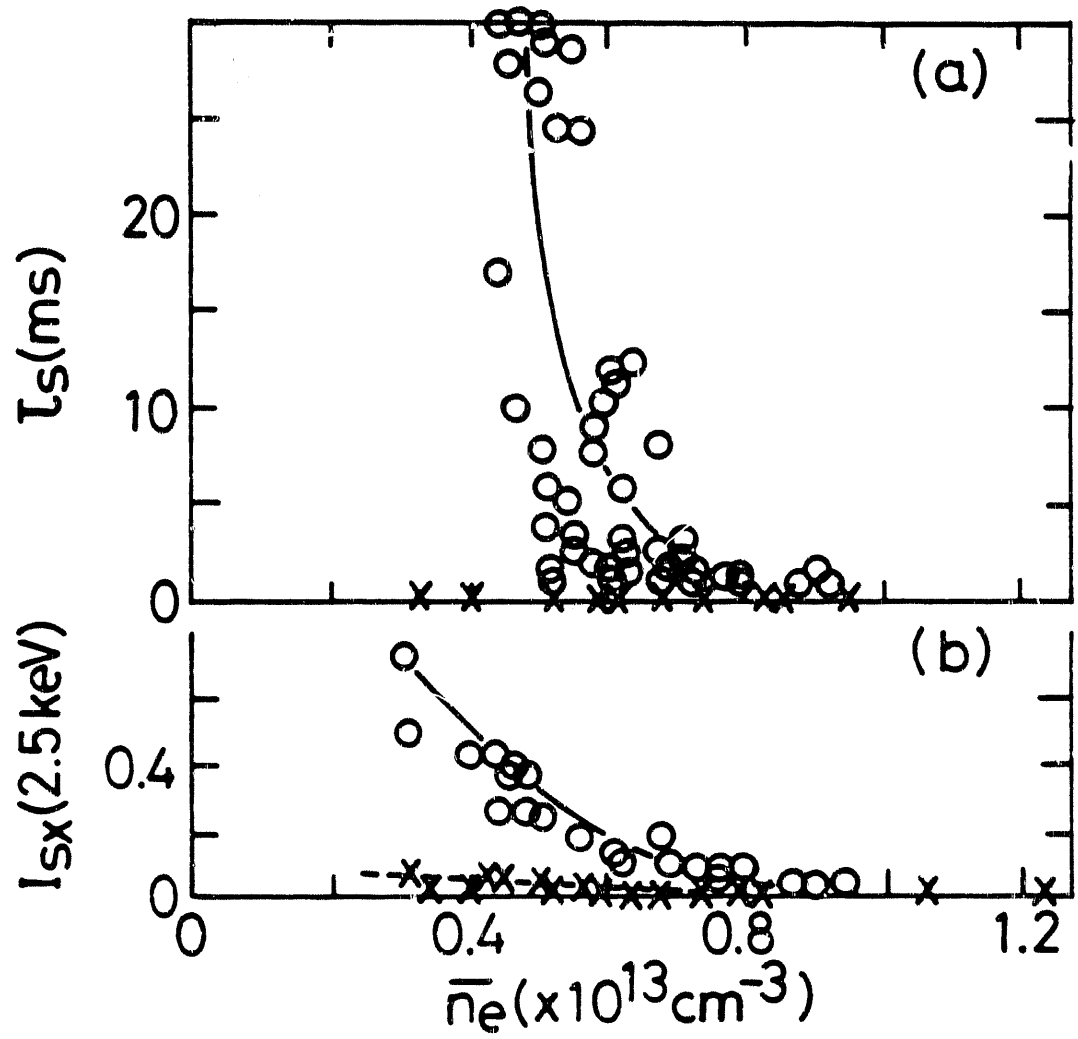


FIG. 4

90x3218

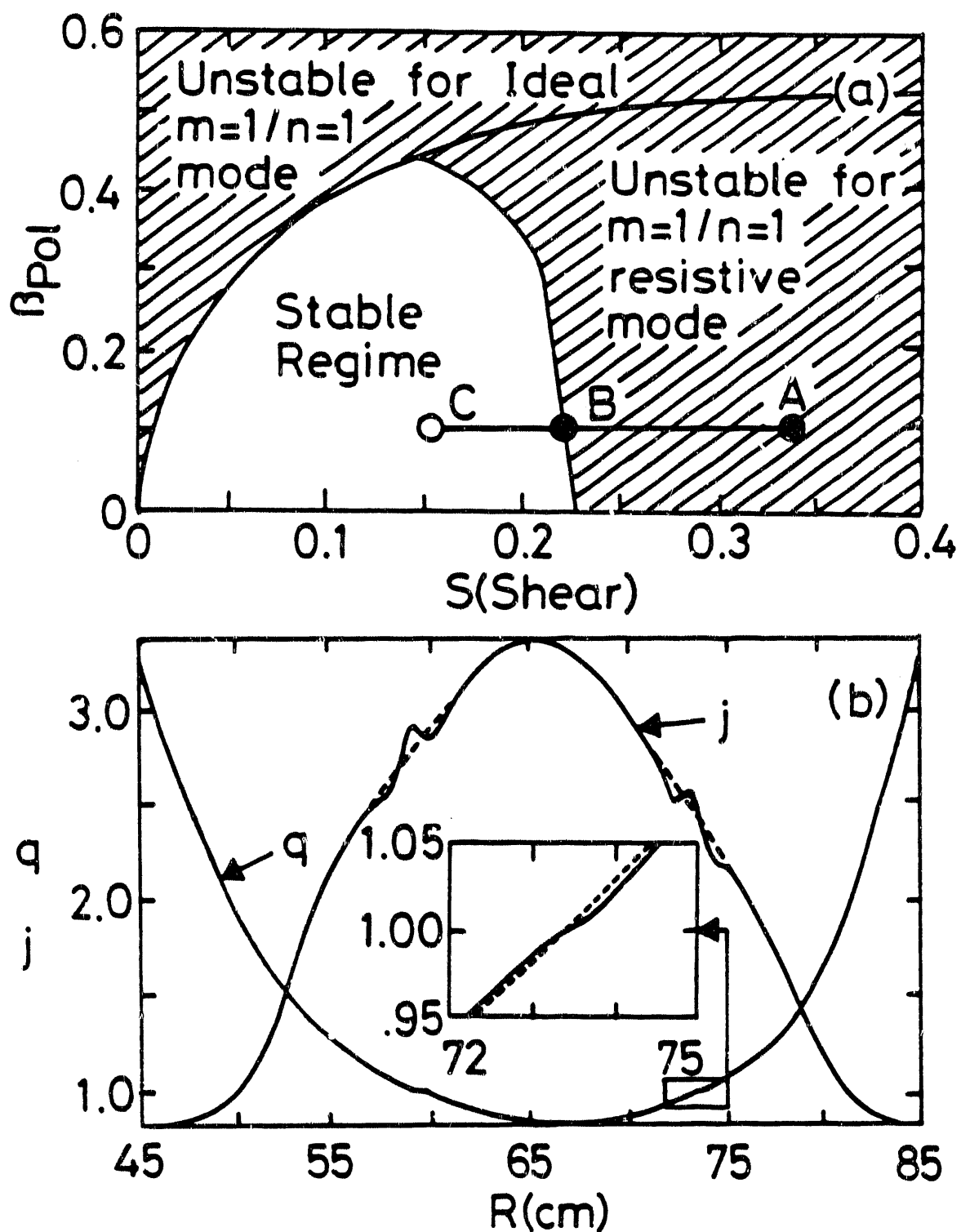


FIG. 5

END

DATE FILMED

12/20/90

